

Simple Book Example

TeXstudio Team

January 2013

ii

thesis

Chapter 1

Light Field Microscope

In this chapter we will explain how the experience acquired running the wave optics simulations of a plenoptic imaging system has been used to design and build a working setup of a light field microscope. The system has been designed for research purpose without thinking to any particular application. It is a versatile and flexible instrument with the purpose to test and explore all the potentials of a light field imaging for microscopy, hence the philosophy behind this project was to realize a setup with the maximum number of degrees of freedom possible. In the next sections we will explain the design parameters and guidelines used to develop setup. A protocol to acquire and render images will be described and few examples of rendered images will be shown.

1.1 From simulation to the real system

The results obtained in the simulation has been used as a guideline in the process of developing a working system. It has been clear since the beginning that a 1.0 system could not be the best option for a practical setup. The

reasons for that are:

- A plenoptic 1.0 imaging system, as explained in ??, requires the lens let array to be conjugated to the object plane, and the sensor plane to be conjugated with the main lens. To satisfy this condition along with the f-number matching, the micro array should be placed at a distance to the sensor equal to its focal length with great precision [2, 10, 8, 4]. A very little tolerance is needed in positioning the micro lens array in order to have a reliable instrument. Advanced machinery and a clean room is needed to fabricate the lens let array with a focal length equal to the substrate thickness and then stick it to the sensor. A solution to bypass this issue is to build a relay system of lenses between the micro lens array and the sensor[7] adding complexity and costs to the system.
- The spatial resolution is limited by the number of lens let in the array. Therefore to achieve high resolution images it is necessary to have small and array with a small pitch and a large number of lens let. The sensor should be as well large enough with small pixel size, increasing the costs. For example to achieve a resolution of 1000 by 1000 pixel in the final rendered image with lens lets with a diameter of $150 \mu\text{m}$ like the one used in section ??, the array should be 15 by 15 cm wide and the sensor should have a resolution of 30000 by 30000 pixel.

Hence from a practical point of view building a proper plenoptic 1.0 system can be quite expensive and complicated respect the performances achieved. A Plenoptic 2.0 instead it is easier to build and gives better results in terms of spatial and directional resolution trade off. The only care it needs regards

the position of the micro lens array respect the sensor.

1.2 Description of the System

In this section it will be described the characteristics of the plenoptic 2.0 microscope built. It has been designed following the line guides given by Georgiev *et al.* [9] for its plenoptic camera. The assembly of the system has been doing using Linos mounts, rods and rails [47]. With reference to figure, the system worked in transmission, and it is composed by three main part:

- Illumination: is made of an LED light, a diffuser and a condensing lens to concentrate the maximum area of the light source on the sample, A Köhler illumination lens has been added in order to generate a even illumination on the sample removing artefacts generated by imaging the light source on the sensor. This illumination solution has been designed by August Köhler in 1893 [48, 49]
- The main optics: its role is to form an image of the object in front of the micro lens array. In our case, like in the simulation, this was a simple 2f system, with a single lens.
- Micro lens array: The micro lens array is a relay system between the main lens image and the sensor of the microscope. It defines the tradeoff between optical and spatio-angular resolution.
- Sensor plane: it records the light field. It should be large enough to capture all the light coming from the lens let array and it should provide enough resolution to have high resolution sub images.

The illumination system was made by an LED light source, Thorlabs LED array LIU630, with a central wavelength of 630 nm , an output power of 208 mW and an emission spectrum shown in figure 1.1 with a full width half maximum of 20 nm as already discussed in ??.

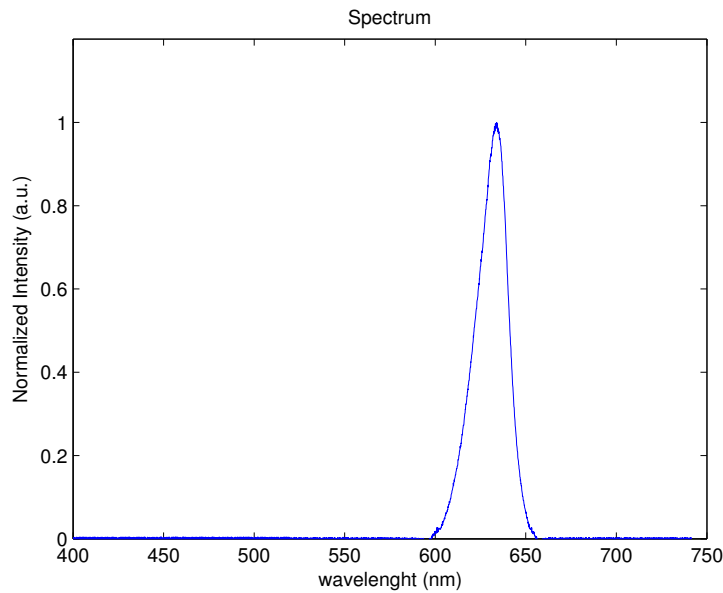


Figure 1.1: Emission spectrum of the LED light source used in the system .

A condensing lens with a focal length of 27 mm has been placed in front of the light source, in order to maximise the light reaching the sample. The image formed by the condensing lens has been relayed by the Köhler lens on the main lens of the system. In this way the structure of the light source is not affecting the quality of the image [48]. To make it even more uniform a diffuser has been placed between the LED source and the condensing lens, as shown in figure 1.2. The main optics consisted of two Linos singlets plano-convex lenses with a focal length of 120 mm each placed one next to the other as shown in figure 1.2, in order to give a main lens with a total focal

length of 60 mm. The two lenses have been mounted with the flat surface facing outwards to minimize spherical aberrations. The main lens was in a 2f configuration, producing a an image with a magnification of 1 on the main lens image plane.

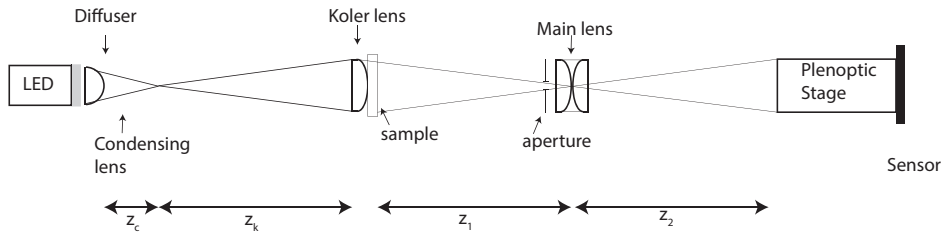


Figure 1.2: Schematics of the light field microscope. The values of the distances are: $z_c=27$ mm, $z_k=120$ mm, $z_1=z_2=120$ mm.

The plenoptic stage is the most complex part of the system. The optical properties are defined by the magnification of the micro array stage [36, 3], therefore in a real system it should be tuned with high accuracy in order to produce a rendered image with the desired resolution. The issue in tuning correctly the magnification is about defining a correct values for the lengths a and b in a real system. The technical solution that has been adopted was to use two micro metric mechanical translation stages to move with precision both the whole micro array and sensor block respect the main lens and the micro array respect the sensor. The first translation stage moves the whole plenoptic block, respect the main lens, changing the parameter a , distance between the man lens image and the micro lens array. Once a is set a second translation stage moves the sensor respect the micro array stage, setting the parameter b , distance between the micro array and the sensor. In this way the magnification is set. The micro array can also be moved perpendicularly

to the optical axis in x and y, in order to centre the array with the sensor.

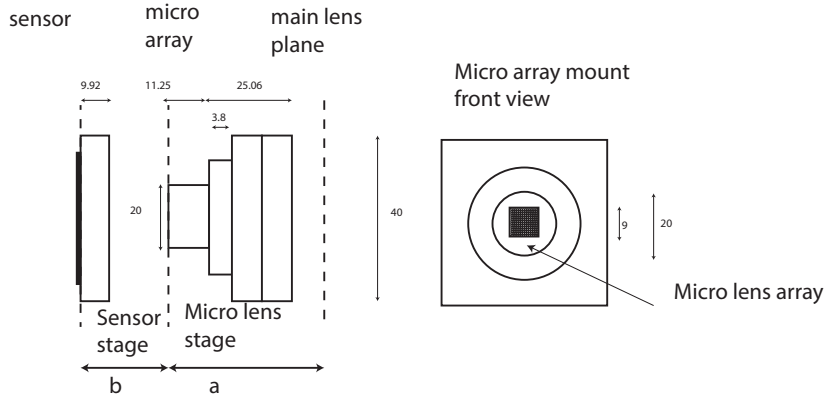


Figure 1.3: Schematics of the light field recording stage.

The micro array used was an MLA150-5c-M by Thorlabs, with a 10 mm by 10 mm square grid made of 146 μm diameter plano-convex lens lets on a substrate of fused silica.. The lens let pitch was 150 μm . All the geometric parameters of the lens let array can be seen in figure 1.4 where r is the radius of curvature of the lens let, s is the high of the lens let from the substrate, p is the pitch, t the thickness of the substrate and f is the focal length that is linked to the radius of curvature by the relation:

$$f = \frac{r}{n - 1} \quad (1.1)$$

Where n is the refractive index of the lens let and the substrate, in case of fused silica is 1.5. Assuming the diameter of the lens let almost equal to the pitch, the radius of curvature is linked to the other geometrical parameters by the relation [35]:

$$r = \frac{s^2 + \frac{p^2}{4}}{2s} \quad (1.2)$$

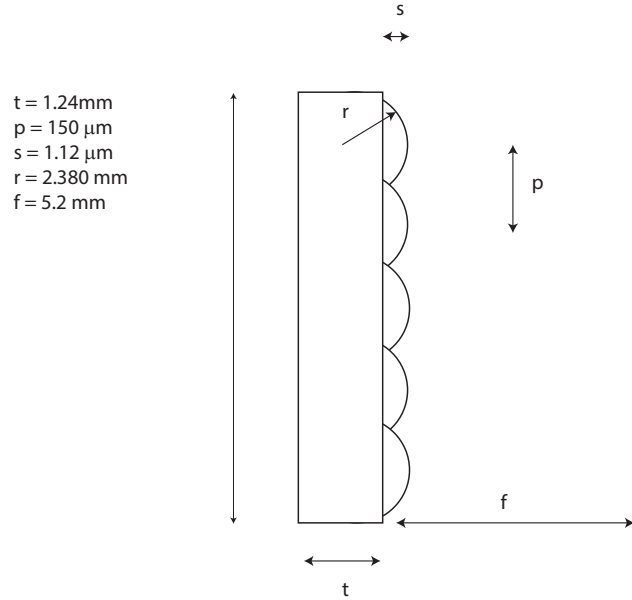


Figure 1.4: Len let array parameters.

The position of the lens let array respect the sensor and the main lens is controlled by two micro metric translation stages. The parameters to control them of the micro lens array are resumed in table 1.2. α and β are in this case the amount of shift that the two translation stages should undergo simultaneously in order to obtain the magnification desired. For each couple (α, β) are shown the optical parameters correspondent: the f-number $F/\#$, the numerical aperture NA the cut-off frequencies of the main lens and of the plenoptic stage ν . To record the raw image has been used a 10 megapixel cmos technology sensor with 3840 by 2748 pixels extracted by a UI-1490LE-C-HQ camera from IDS Imaging Development System GmbH. Pixel where $1.67 \mu\text{m}$ with a sensor size of 6.413 mm by 4.589 mm.

CHAPTER 1. LIGHT FIELD MICROSCOPE

Magnification	a (m)	b (m)	NA	F#	ν Main lens (cycle/m)	ν Plenoptic (cycle/m)	α (m)	β (m)
0	0	0.0052	0.014423077	34.66666667	22785.2716	0	0.0052	0
0.1	0.0572	0.00572	0.013111888	38.13333333	20713.88327	0.00572	0.05148	
0.15	0.039866667	0.00598	0.012541806	39.86666667	19813.27965	2971.991948	0.00598	0.033886667
0.2	0.0312	0.00624	0.012019231	41.6	18987.72633	3797.545267	0.00624	0.02496
0.25	0.026	0.0065	0.011538462	43.3333333	18228.21728	4557.05432	0.0065	0.0195
0.3	0.022533333	0.00676	0.011094675	45.06666667	17527.132	5258.1396	0.00676	0.015773333
0.35	0.020057143	0.00702	0.010683761	46.8	16877.97896	5907.292637	0.00702	0.013037143
0.4	0.0182	0.00728	0.010302198	48.53333333	16275.194	6510.0776	0.00728	0.01092
0.45	0.016755556	0.00754	0.00994695	50.26666667	15713.98041	7071.291186	0.00754	0.009215556
0.5	0.0156	0.0078	0.009615385	52	15190.18107	7595.090533	0.0078	0.0078
0.55	0.014654545	0.00806	0.009305211	53.7333333	14700.17523	8085.096374	0.00806	0.006594545
0.6	0.013866667	0.00832	0.009014423	55.46666667	14240.79475	8544.47685	0.00832	0.00546667
0.65	0.0132	0.00858	0.008741259	57.2	13809.25552	8976.016085	0.00858	0.00462
0.7	0.012628571	0.00884	0.008484163	58.9333333	13403.10094	9382.170659	0.00884	0.003788571
0.75	0.012133333	0.0091	0.008241758	60.66666667	13020.1552	9765.1164	0.0091	0.003033333
0.8	0.0117	0.00936	0.008012821	62.4	12658.48422	10126.78738	0.00936	0.00234
0.85	0.011317647	0.00962	0.007796258	64.1333333	12316.36303	10468.90857	0.00962	0.001697647
0.9	0.01097778	0.00988	0.007591093	65.86666667	11922.24821	10793.02339	0.00988	0.001097778
0.95	0.010673684	0.01014	0.00739645	67.6	11684.75467	11100.51693	0.01014	0.000533684
1	0.0104	0.0104	0.007211538	69.33333333	11392.6358	0.0104	0	

Table 1.1: Table containing the parameters of the micro lens array translation stage. a and b are the distances shown in figure 1.4, while α and β are the shift that the micro metric translator should be moved. In the tables are shown also the optical parameters corresponding to the different positions of the translator.

1.3 Performances of the system

In parallel with what has been said in section ??, we can define the theoretical performances parameters for the real system designed after the simulated one.

In table 1.2 are shown the Numerical aperture, and F-number of the system according to the magnification obtained tuning distances a and b . It is also shown the correspondent optical resolution ν main lens and ν plenoptic. The values of plenoptic optical resolution are plotted in figure

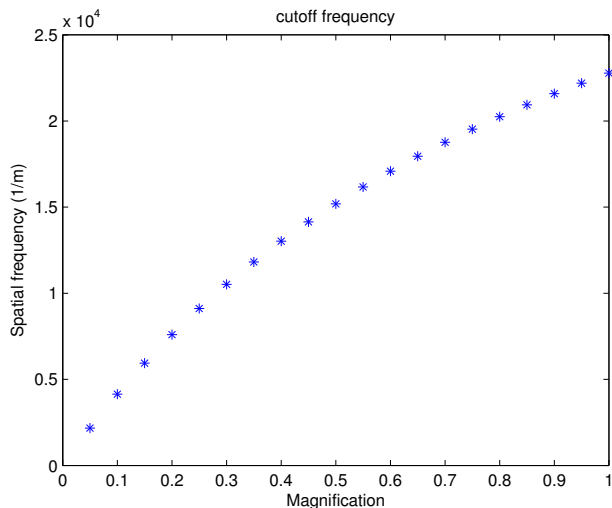


Figure 1.5: Optical resolution as a function of the magnification.

The optical resolution is expected to drop with the decrease of the magnification.

1.4 Image acquisition protocol

A protocol to capture plenoptic raw data from the system built has been developed. the protocol can be resumed in the following steps:

- according to the magnification required the parameters a and b are setted moving the two translation stages of the quantities α and β indicated in table 1.2.
- A calibration image is captured removing the sample and imaging an uniform pattern of monochromatic light.
- The sample is put back in place and the raw imaged is captured.
- The final image is rendered using the basic rendering algorithm explained in section ??.

The reason to acquire the calibration image is to verify the correct alignment of the lens let array, to match the matching the f-number and to have a guide to create the sub-images grid to render the final image. The micro array could be off axis and not aligned with the sensor boundaries. The position in x and y of the micro lens array can be adjusted moving the mount of the micro array in x and y until the round sub images are aligned with the frame of the field of view and rotating the array around the optical axis. The same image can be used to match the f-number of the main lens with the one of the lens let array according to the configuration of a and b chosen. This is done manually changing the aperture placed in front of the main lens until the white spots of the sub images touches each other. In figure 1.6 it is shown the case where the aperture of the main lens is too small, and the gap between the sub images is too large. In figure 1.7 is shown the calibration image obtained with the correct aperture of the main lens.

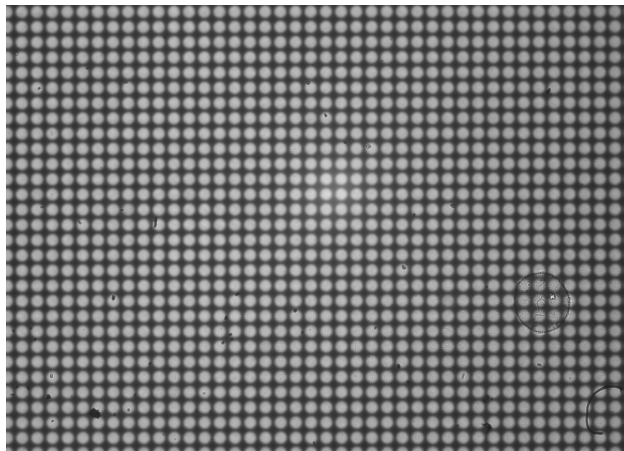


Figure 1.6: Calibration image with f-number not matched.

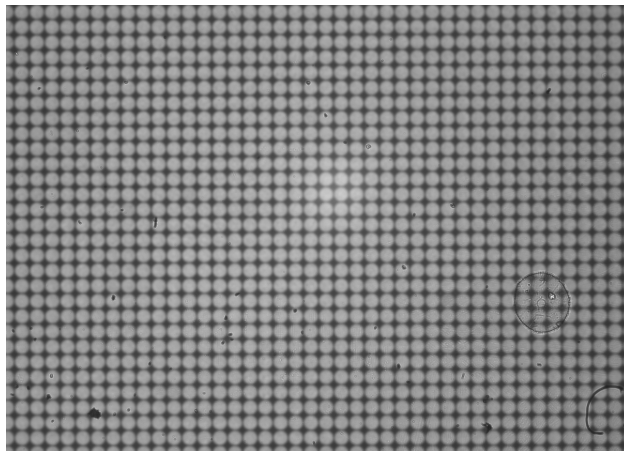
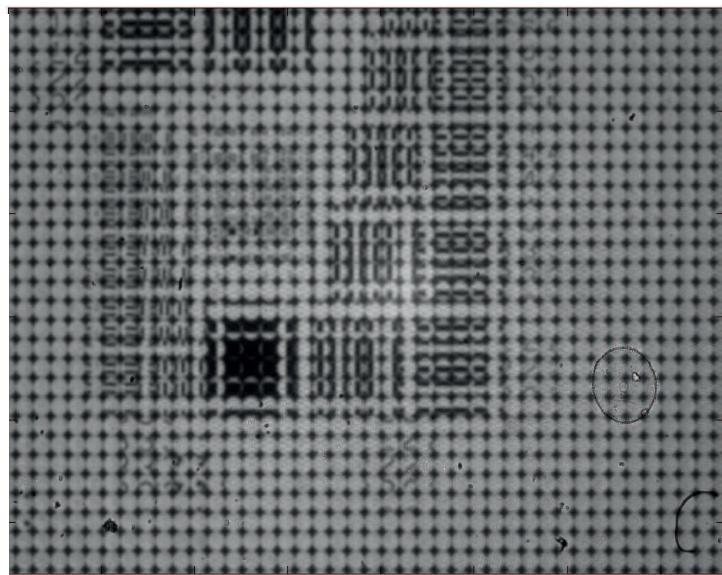


Figure 1.7: Calibration image with matched f-number.

After the f-number is matched, it is possible to proceed with the acquisition of the raw image of the sample. In this case a USAF resolution target has been used as an object. In figure 1.8 are shown the raw images obtained with magnifications equal to 0.5 and 0.4, while in figure 1.9 are shown the raw images obtained with a magnification of 0.3 and 0.25.

Magnification: 0.5



Magnification: 0.4

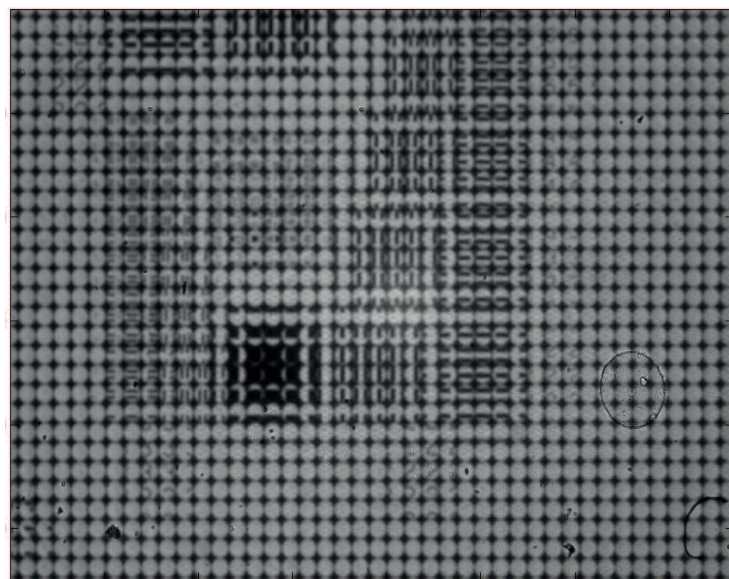
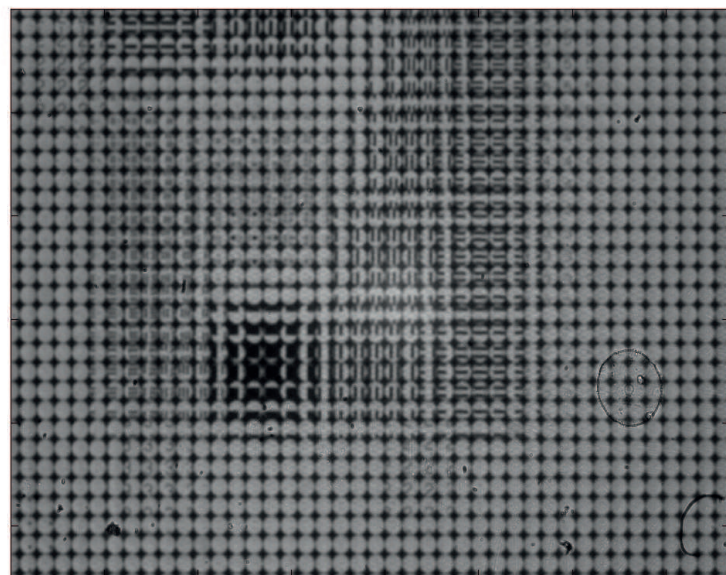


Figure 1.8: Calibration image with matched f-number.

Magnification: 0.3



Magnification: 0.25

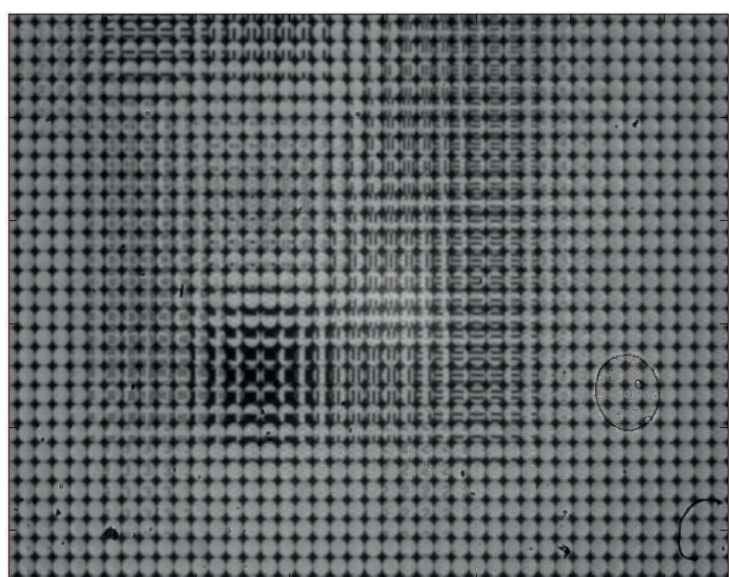


Figure 1.9: Calibration image with matched f-number.

From this raw images is evident how the different features of the target object are decomposed into sub images. The number of sub images into it is decomposed increase with the decrease of the magnification. The algorithm to extract the rendering grid will by the calibration image will be explained in the next section.

1.5 Rendering of experimental data

Rendering images from raw data acquired by a real light field microscope is more complicated than the case of the simulates raw data. While in a simulation the lens let array is perfectly aligned with the other optical components, in a real system this is not true any more. The lens let array can have a small tilt respect the plane perpendicular to the optical axis, causing small differences in magnification along the sub image grid. When this happen the sub images will have different size along the grid, generating a distortion that is not predictable or quantifiable like in the case of the computer generated raw data in section ???. For this reason an algorithm to extract the information on the position of the sub images from the calibration image has been elaborated. It is made by the following steps as shown in figure :

- The user selects a row and a column of sub images in calibration image corresponding to the raw image to render
- the intensity profile of the row and the column are displayed and the user sets a threshold that will be used by the software to discriminate the boundaries of the sub images.
- a grid is formed in correspondence with the detected sub images

- the grid is shown superimposed to the calibration image. Usually offsets are presents and are removed manually by the user.
- the image is rendered as explained in section ?? using the grid created from the calibration image.

The final rendered images can be seen in figure 1.11.

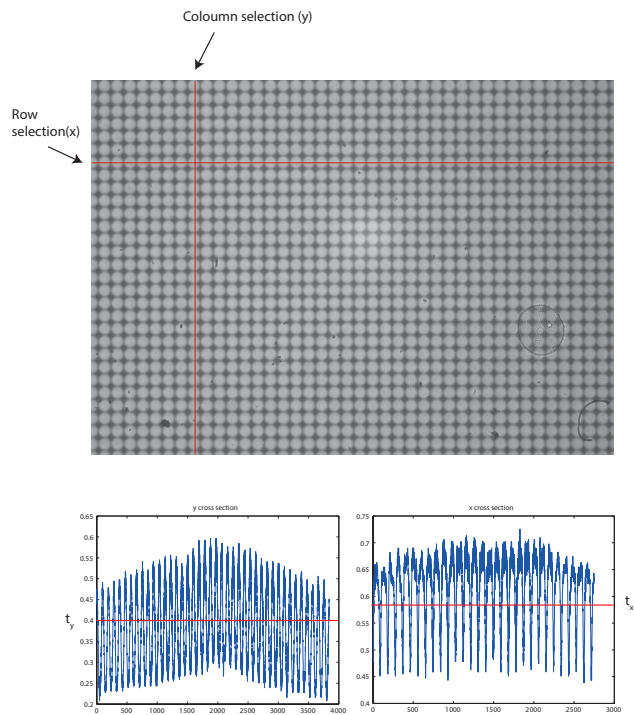


Figure 1.10: The sub images grid is made selecting a row and a column from the calibration image and setting a threshold to that allows the software to know when a sub image ends and the other end.

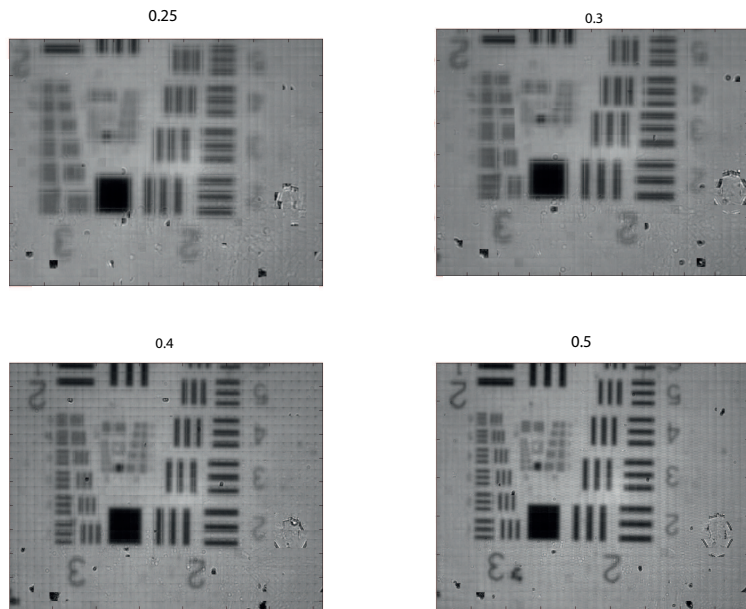


Figure 1.11: Rendered image from the raw data shown in figures 1.8 and 1.9. Magnifications are from top left to bottom right: 0.25 0.3 0.4 and 0.5.

As expected from the simulated data and the theory of diffraction, resolution drops dramatically with the magnification. From a qualitative analysis, the image gets more blurred for low magnification values, in agreement with what seen in previous chapters.

Chapter 2

Conclusions and Future work

Bibliography

- [1] Shree K Nayar. Computational cameras: Redefining the image. *Computer*, (8):30–38, 2006.
- [2] Ren Ng. *Digital light field photography*. PhD thesis, stanford university, 2006.
- [3] Todor Georgiev and Andrew Lumsdaine. Focused plenoptic camera and rendering. *Journal of Electronic Imaging*, 19(2):021106–021106, 2010.
- [4] Levoy Mark. Stanford light field microscope project, 2005.
- [5] Changyin Zhou and Shree K Nayar. Computational cameras: Convergence of optics and processing. *Image Processing, IEEE Transactions on*, 20(12):3322–3340, 2011.
- [6] Edward H Adelson and James R Bergen. *The plenoptic function and the elements of early vision*. Vision and Modeling Group, Media Laboratory, Massachusetts Institute of Technology, 1991.
- [7] Edward H Adelson and John Y. A. Wang. Single lens stereo with a plenoptic camera. *IEEE Transactions on Pattern Analysis & Machine Intelligence*, (2):99–106, 1992.

- [8] Marc Levoy and Pat Hanrahan. Light field rendering. In *Proceedings of the 23rd annual conference on Computer graphics and interactive techniques*, pages 31–42. ACM, 1996.
- [9] Todor Georgiev and Chintan Intwala. Light field camera design for integral view photography. *Adobe System, Inc*, 2006.
- [10] Ren Ng, Marc Levoy, Mathieu Brédif, Gene Duval, Mark Horowitz, and Pat Hanrahan. Light field photography with a hand-held plenoptic camera. *Computer Science Technical Report CSTR*, 2(11), 2005.
- [11] Andrew Lumsdaine and Todor Georgiev. Full resolution lightfield rendering. *Indiana University and Adobe Systems, Tech. Rep*, 2008.
- [12] Andrew Lumsdaine and Todor Georgiev. The focused plenoptic camera. In *Computational Photography (ICCP), 2009 IEEE International Conference on*, pages 1–8. IEEE, 2009.
- [13] Victor Guillemin and Shlomo Sternberg. *Symplectic techniques in physics*. Cambridge University Press, 1990.
- [14] Todor Georgiev, Andrew Lumsdaine, and Sergio Goma. Plenoptic principal planes. In *Imaging Systems and Applications*, page JTuD3. Optical Society of America, 2011.
- [15] Arnold Sommerfeld. Optics lectures on theoretical physics, vol. iv. *Optics Lectures on Theoretical Physics, Vol. IV by Arnold Sommerfeld New York, NY: Academic Press INC, 1954*, 1, 1954.

- [16] Joseph W Goodman. *Introduction to Fourier optics*. Roberts and Company Publishers, 2005.
- [17] Maciej Sypek. Light propagation in the fresnel region. new numerical approach. *Optics communications*, 116(1):43–48, 1995.
- [18] Rafael C Gonzalez, Richard Eugene Woods, and Steven L Eddins. *Digital image processing using MATLAB*. Pearson Education India, 2004.
- [19] Kyoji Matsushima and Tomoyoshi Shimobaba. Band-limited angular spectrum method for numerical simulation of free-space propagation in far and near fields. *Optics express*, 17(22):19662–19673, 2009.
- [20] Maciej Sypek. Reply to the comment on “light propagation in the fresnel region–new numerical approach”. *Optics Communications*, 282(6):1074–1077, 2009.
- [21] Max Born and Emil Wolf. *Principles of optics: electromagnetic theory of propagation, interference and diffraction of light*. Cambridge university press, 1999.
- [22] Joseph W Goodman and Randy L Haupt. *Statistical optics*. John Wiley & Sons, 2015.
- [23] Emil Wolf. *Introduction to the Theory of Coherence and Polarization of Light*. Cambridge University Press, 2007.
- [24] Frank L Pedrotti and Leno S Pedrotti. Introduction to optics 2nd edition. *Introduction to Optics 2nd Edition by Frank L. Pedrotti, SJ, Leno S. Pedrotti New Jersey: Prentice Hall, 1993, 1, 1993*.

- [25] Todor G Georgiev and Andrew Lumsdaine. Resolution in plenoptic cameras. In *Computational Optical Sensing and Imaging*, page CTuB3. Optical Society of America, 2009.
- [26] Todor Georgiev and Andrew Lumsdaine. Superresolution with plenoptic camera 2.0. *Adobe Systems Incorporated, Tech. Rep*, 2009.
- [27] Gordon Wetzstein, Ivo Ihrke, Douglas Lanman, and Wolfgang Heidrich. Computational plenoptic imaging. In *Computer Graphics Forum*, volume 30, pages 2397–2426. Wiley Online Library, 2011.
- [28] Todor G Georgiev and Andrew Lumsdaine. Super-resolution with the focused plenoptic camera, November 20 2012. US Patent 8,315,476.
- [29] Tom E Bishop, Sara Zanetti, and Paolo Favaro. Light field superresolution. In *Computational Photography (ICCP), 2009 IEEE International Conference on*, pages 1–9. IEEE, 2009.
- [30] Todor Georgiev. Plenoptic camera resolution. In *Computational Optical Sensing and Imaging*, pages JTh4A–2. Optical Society of America, 2015.
- [31] Todor Georgiev, Ke Colin Zheng, Brian Curless, David Salesin, Shree Nayar, and Chintan Intwala. Spatio-angular resolution tradeoffs in integral photography. *Rendering Techniques*, 2006:263–272, 2006.
- [32] Christian Perwass and Lennart Wietzke. Single lens 3d-camera with extended depth-of-field. In *Proc. SPIE*, volume 8291, page 829108, 2012.
- [33] Michael Hansen and Eric Holk. Depth map estimation for plenoptic images. 2011.

- [34] Ole Johannsen, Christian Heinze, Bastian Goldluecke, and Christian Perwass. On the calibration of focused plenoptic cameras. In *Time-of-Flight and Depth Imaging. Sensors, Algorithms, and Applications*, pages 302–317. Springer, 2013.
- [35] Hans Peter Herzig. *Micro-optics: elements, systems and applications*. CRC Press, 1997.
- [36] Massimo Turola and Steve Gruppetta. Wave optics simulations of a focused plenoptic system. In *Frontiers in Optics*, pages JTU3A–24. Optical Society of America, 2014.
- [37] Todor Georgiev and Andrew Lumsdaine. The multifocus plenoptic camera. In *IS&T/SPIE Electronic Imaging*, pages 829908–829908. International Society for Optics and Photonics, 2012.
- [38] Todor Georgiev, Georgi Chunev, and Andrew Lumsdaine. Superresolution with the focused plenoptic camera. In *IS&T/SPIE Electronic Imaging*, pages 78730X–78730X. International Society for Optics and Photonics, 2011.
- [39] Todor G Georgiev, Andrew Lumsdaine, and Sergio Goma. High dynamic range image capture with plenoptic 2.0 camera. In *Signal recovery and synthesis*, page SWA7P. Optical Society of America, 2009.
- [40] Paolo Favaro. A split-sensor light field camera for extended depth of field and superresolution. In *SPIE Photonics Europe*, pages 843602–843602. International Society for Optics and Photonics, 2012.

- [41] Tom E Bishop and Paolo Favaro. The light field camera: Extended depth of field, aliasing, and superresolution. *Pattern Analysis and Machine Intelligence, IEEE Transactions on*, 34(5):972–986, 2012.
- [42] Tom E Bishop and Paolo Favaro. Full-resolution depth map estimation from an aliased plenoptic light field. In *Computer Vision–ACCV 2010*, pages 186–200. Springer, 2011.
- [43] Sapna Shroff and Kathrin Berkner. High resolution image reconstruction for plenoptic imaging systems using system response. In *Computational Optical Sensing and Imaging*, pages CM2B–2. Optical Society of America, 2012.
- [44] Sapna A Shroff and Kathrin Berkner. Image formation analysis and high resolution image reconstruction for plenoptic imaging systems. *Applied optics*, 52(10):D22–D31, 2013.
- [45] Chien-Hung Lu, Stefan Muenzel, and Jason Fleischer. High-resolution light-field microscopy. In *Computational Optical Sensing and Imaging*, pages CTh3B–2. Optical Society of America, 2013.
- [46] Vivek Boominathan, Kaushik Mitra, and Ashok Veeraraghavan. Improving resolution and depth-of-field of light field cameras using a hybrid imaging system. In *Computational Photography (ICCP), 2014 IEEE International Conference on*, pages 1–10. IEEE, 2014.
- [47] Photonics for Innovations Quioptiq. *The Linos Catalog*. 2015.

- [48] August Köhler. A new system of illumination for photomicrographic purposes. *Z. Wiss. Mikroskopie*, 10:433–440, 1893.
- [49] August Kohler and Walter Bauersfeld. Device for light-field and dark-field illumination of microscopic objects, January 16 1934. US Patent 1,943,510.